A SIMPLIFIED MODEL FOR FUEL ISOTOPE EVOLUTION IN ATW SYSTEMS - LIQUID METAL COOLED FAST REACTOR -

M. Cheon, J. Ahn, E. Greenspan, D. Barnes, and P. L. Chambré
Department of Nuclear Engineering
University of California
Berkeley, CA 94720
mgcheon@nuc.berkeley.edu, ahn@nuc.berkeley.edu

ABSTRACT

A simplified model and computer code have been developed for the simulation of the evolution of the fuel inventory in accelerator-driven transmutation of waste (ATW) systems, taking into account constraints on the reactor core design. The model and code developed has been found to be in good agreement with results obtained with MOCUP. The application of the newly developed tool is illustrated for the proposed ATW blanket point design. The design and performance characteristics provided by the new tool include the cycle dependent inventory of fuel required for a prescribed value of k_{eff} at the beginning of a cycle. For a given Δk_{eff}, the cycle duration is determined. Based on the compositions of the discharged fuel, the fractional transmutation, the cumulative waste reduction ratio, and the cumulative toxicity reduction ratio are calculated. It is estimated that the fuel loading and cycle duration of a lead-bismuth cooled transmuting reactor will keep increasing over the first few dozen cycles, if k_{eff} the control is achieved by adjusting the actinides-to-zirconium volume ratio. With the recycle system studied, the toxicity of the light-water reactor spent fuel is reduced by a factor of hundred.

1. INTRODUCTION

Several types of accelerator-driven transmutation of waste (ATW) systems are currently being examined as options for processing spent fuel from Light-Water Reactors (LWRs). The primary function of the ATW system is to transmute transuranics (TRU) and long-lived fission products into short-lived, less toxic nuclides so as to reduce the amount and the toxicity of the high-level waste (HLW) to be sent to repositories. In the process it will utilize the energy produced from the fissioning of the actinides for generating electricity. A liquid-metal (LM) cooled reactor is one of the leading reactor technologies being considered for the ATW system [1,2].

The evaluation of the performance characteristics of the transmutation system requires multi-cycle analysis of the reactor and fuel cycle facilities. There are several general purpose reactor analysis code systems that can perform multi-cycle burnup analysis. Examples of such code systems are REBUS-3 developed at ANL [3], MOCUP developed at INEEL [4] and MONTEBURNS recently developed at LANL [5]. The latter two code systems use the ORIGEN 2 code developed by ORNL [6] for the burnup analysis. Some of the available code systems, such as REBUS-3, can automatically find the fuel composition in the equilibrium cycle. However, applying the available design codes to study the time evolution of the fuel constituents in the ATW system requires significant effort and computer time. The effort is particularly demanding if the analysis is to include re-designing the core each cycle so as to get a given value of k_{eff} (say, 0.98) for the beginning of cycle (BOC) and another given value of k_{eff} (say, 0.92) at the end of cycle (EOC).

The purposes of the present work are (1) to develop a simplified fuel cycle analysis tool that will enable to perform multi-cycle burnup analysis in a short time while accounting for the BOC and EOC k_{eff} constraints, and (2) to develop a tool that will couple the transmuting reactor performance analysis, out-of-core fuel cycle analysis and the repository performance analysis. The developed tool is intended primarily for scoping studies that compare different designs and mode of operation of ATW systems from the viewpoint of waste impact reduction.

The mathematical model developed is described in Sec. 2 and its benchmarking against MOCUP is described in Sec. 3. Illustrations of the information on the ATW system performance that can be obtained with the developed tool are presented in Sec. 4.

2. ANALYTICAL MODEL

We consider an ATW fuel cycle, shown in Figure 1. This ATW fuel cycle consists of an ATW-reactor, a partitioning plant, a fuel-fabrication facility, a makeup material storage, and a repository. Actinides are assumed to be recovered from the discharged fuel by the partitioning plant and passed through the fabrication plant before recycling. A *cycle* starts at the beginning of irradiation in the reactor. At the end of one irradiation period, the fraction, *f,* of the fuel in the core is discharged and partitioned. Recovered actinides are mixed with makeup materials (actinides and zirconium) and fabricated into fuel, which is returned to the reactor core. This is the point where one cycle ends. This cycle is repeated many times.

The model is based on the following assumptions: (1) The reactor core is homogenized. (2) Partitioning of the discharged fuel and the fabrication are done instantaneously. Waste generation from the fabrication plant is neglected. (3) Only actinides are recovered, and all isotopes of element *e* are assumed to have the same recovery fraction, R_e. Recovery fraction is defined in Sec. 2.2. (4) The recharged fuel is mixed instantaneously and homogeneously with the fuel that stays in the core. (5) The reactor is operated at a constant power. (6) The fission products (FP) effect on k_{eff} is accounted for by considering a fictitious FP pair. (7) Effective one-group cross sections are used for reaction rate calculations. These are generated by MCNP [7] for the representative core composition and assumed to be constant within a cycle. (8) The total fuel volume in the reactor is constant. (9) The actinides-to-Zr ratio is adjusted at each beginning of the cycle (BOC), so that the BOC k_{eff} will be 0.98. (10) The cycle terminates when k_{eff} drops to 0.92.

The present model can be divided into two parts: (1) determination of the fuel composition by nuclear reactions and decays in the reactor core and (2) determination of fuel composition after partitioning, fabrication, and reloading.

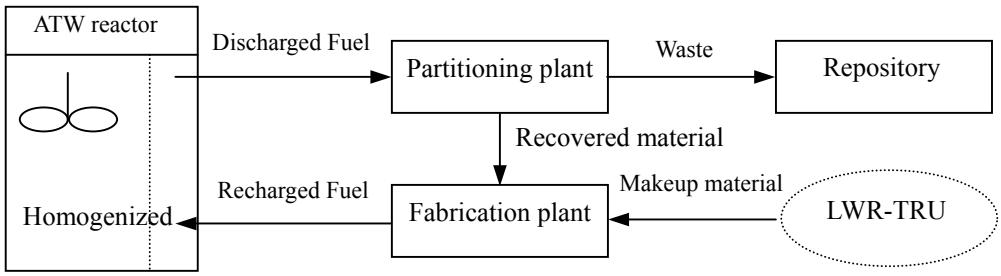

Figure 1.Simplified ATW fuel cycle

2.1 REACTOR MODEL

For the determination of fuel compositions in the reactor, we have developed a model to calculate the inventory of ^{234}U, ^{235}U, ^{236}U, ^{238}U, ^{237}Np, ^{238}Pu, ^{239}Pu, ^{240}Pu, ^{241}Pu, ^{242}Pu, ^{241}Am, ^{242m}Am, ^{243}Am, ^{242}Cm, ^{243}Cm, ^{244}Cm, ^{245}Cm, and ^{246}Cm in the reactor. These nuclides are indexed by *i* from 1 to 18 in this order. Figure 2 shows the 18-nuclide chain considered in this work. The number in the parenthesis of each box shows the nuclide index, *i*. Three types of neutron reactions and four types of decay modes were considered to account for the mass change of a nuclide. If a nuclide captures a neutron, it turns into either a nuclide with the mass number greater by one, emitting a photon, or a nuclide with the mass number smaller by one, emitting two neutrons. These are represented by vertical arrows in Figure 2. Upon neutron absorption, fission may also occur. The fission reaction is represented by an upward diagonal arrow (either up or down) in Figure 2. A downward diagonal arrow represents an alpha decay, while a horizontal arrow indicates a beta (or EC) decay. In Figure 2, the short-lived nuclides, ^{237}U, ^{239}U, ^{238}Np, ^{239}Np, ^{237}Pu, ^{243}Pu, ^{240}Am, ^{242}Am, ^{244}Am, and ^{241}Cm (6.75 day, 23.45 minute, 2.12 day, 2.36 day, 45.2 day, 4.96 hour, 50.8 hour, 16.0 hour, 10.1 hour, and 32.8 day [8], respectively), boxed by dotted lines, are not included explicitly in the present model. It is assumed that they decay into their daughter nuclides immediately.

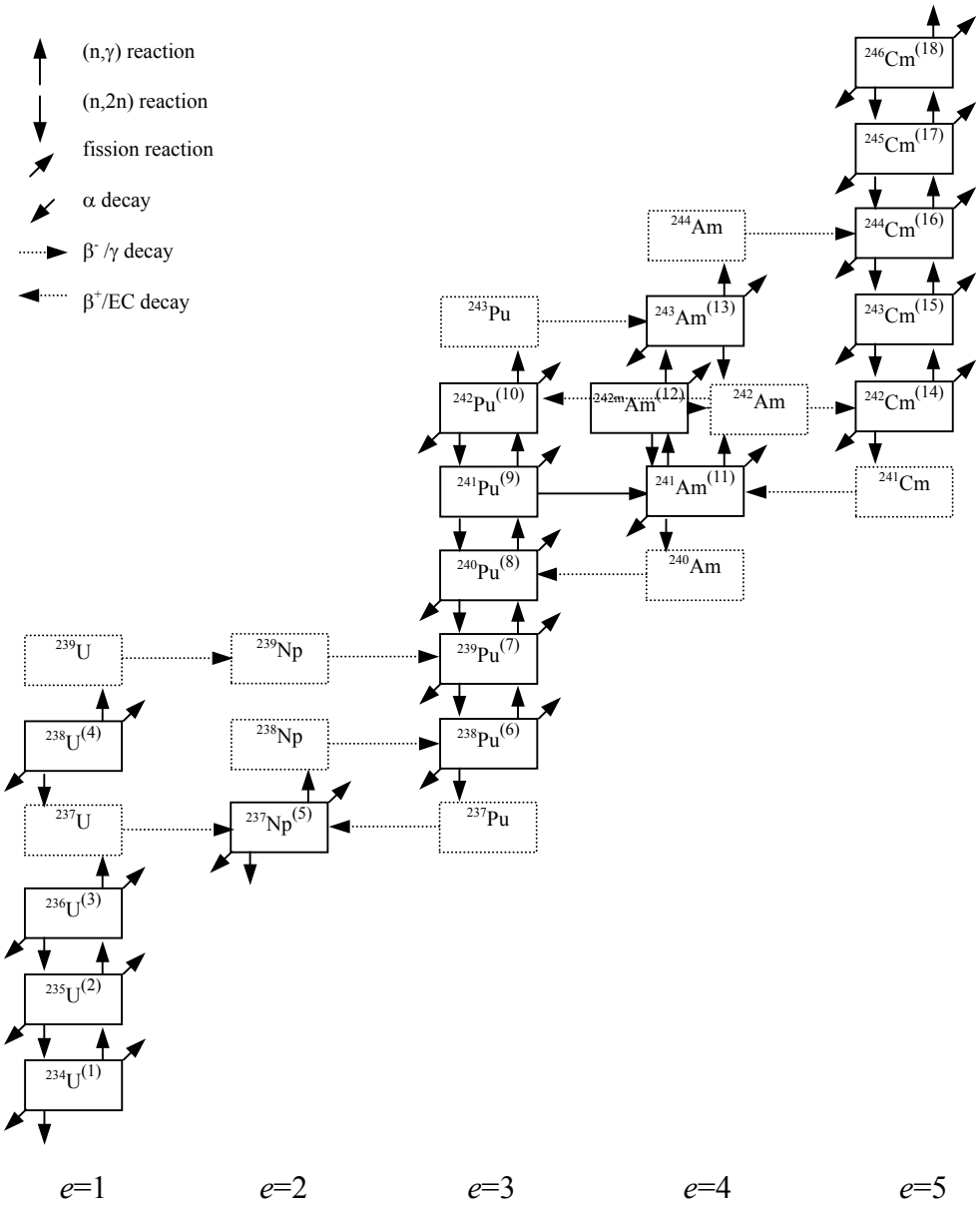

Figure 2. The 18-nuclide chain considered for this study

The composition change in the reactor by the nuclear reactions and decays in the *n*-th cycle is expressed as

$$\frac{d\vec{N}_n(t)}{dt} = \mathbf{D}_n \vec{N}_n(t), \qquad T_n^o \le t \le T_n^o + T_n \equiv T_{n+1}^o, \qquad n=1,2,\ldots,\mathcal{N}, \tag{1}$$

subject to

$$\vec{N}_n(T_n^o) = \vec{N}_n^o, \qquad n=1,2,\ldots,\mathcal{N}, \tag{2}$$

where $\vec{N}_n(t)$ is the vector whose elements express the number of atoms of each nuclide shown in Figure 2 during the irradiation period of the *n*-th cycle. $\vec{N}_n^o$ is the vector for the number of atoms of nuclides in the fuel in the reactor core at the beginning of the irradiation of the *n*-th cycle. *t* is the time after the fuel cycle is started to operate. T_n^o is the time when the *n*-th cycle starts. T_n is the duration of the irradiation in the *n*-th cycle. The

matrix $\mathbf{D_n}$ represents transmutation of nuclides by the reactions with neutrons and decays in the reactor core at the *n*-th cycle, which is shown in Figure 2. If (1) is applied to ^{237}Np for which $i = 5$ (Figure 2) then,

$$\frac{dN_{5,n}(t)}{dt} = -(\overline{\sigma}_{5,a}\phi_n(t) + \lambda_5)N_{5,n}(t) + \overline{\sigma}_{3,\gamma}\phi_n(t)N_{3,n}(t) + \overline{\sigma}_{4,2n}\phi_n(t)N_{4,n}(t) + \overline{\sigma}_{6,2n}\phi_n(t)N_{6,n}(t) + \lambda_{11,\alpha}N_{11,n}(t)\,. \quad (3)$$

$\overline{\sigma}_{i,a}$, $\overline{\sigma}_{i,\gamma}$, $\overline{\sigma}_{i,2n}$, and $\overline{\sigma}_{i,f}$ are the effective one-group cross sections of nuclide *i* for absorption, capture, (n,2n), and fission, respectively. $\lambda_{i,\alpha}$, $\lambda_{i,\beta}$, $\lambda_{i,EC}$, and $\lambda_{i,\gamma}$ are decay constants for α-, β-, EC- and γ-decays for nuclide *i*, respectively. $\phi_n(t)$ is the time-dependent neutron flux at the *n*-th cycle. It is assumed that the number of atoms of zirconium at the *n*-th cycle does not change by the neutron reaction. The production rate of fission-product pairs generated by the fission of actinide atoms at the *n*-th cycle is expressed by

$$\frac{dN_{F,n}(t)}{dt} = \sum_i \sigma_{i,f}\phi_n(t)N_{i,n}(t)\,, \quad (4)$$

where $N_{F,n}(t)$ is the number of fission-product pairs at the *n*-th cycle at time *t* in the reactor. The time-dependent neutron flux is calculated from the expression,

$$\phi_n(t) = \frac{6.242\times10^{18}\,P}{\sum_i \gamma_i \overline{\sigma}_{i,f} N_{i,n}(t)}\,, \quad (5)$$

where γ_i is the recoverable energy of nuclide *i* per fission, and is given by $\gamma_i = 1.29927\times10^{-3}Z^2A^{1/2} + 33.12$ [*MeV*] [9], where *P* is the power [MWt] of the ATW reactor, which is assumed to be constant, and $N_{i,n}(t)$ is the number of atoms of nuclide *i* at the *n*-th cycle at time *t* in the reactor.

To solve (1) numerically, a predictor-corrector scheme has been developed based on Ref. [10]. The size of the time interval for the time marching calculation has been determined such that the relative errors become less than 1/1000.

The irradiation time at the *n*-th cycle, T_n, is determined by bounding the effective multiplication factor, k_{eff}, of the reactor. k_{eff} at the *n*-th cycle is calculated from the expression

$$k_{eff,n} = \frac{\sum_i \eta_i N_{i,n}\overline{\sigma}_{i,a}}{\xi\left(\sum_i N_{i,n}\overline{\sigma}_{i,a} + N_{F,n}\overline{\sigma}_{F,a} + N_{Zr,n}\overline{\sigma}_{Zr,a} + \sum_P N_P\overline{\sigma}_{P,a}\right)}\,, \quad (6)$$

where

$$\eta_i \equiv \frac{\nu_i\overline{\sigma}_{i,f} + \overline{\sigma}_{i,2n}}{\overline{\sigma}_{i,a}}\,, \qquad i=1,2,\ldots,18, \quad (7)$$

ν_i = the average number of neutrons produced per neutron-induced fission in nuclide *i* ,
$\overline{\sigma}_{F,a}$ = the absorption cross-section of a fictitious fission-product pair,
$\overline{\sigma}_{Zr,a}$ = the effective one-group absorption cross-section of zirconium,
$\overline{\sigma}_{P,a}$ = the effective one-group absorption cross-section of an element, *p*, in the structure or the coolant of the reactor, and
ξ = the neutron leakage factor.

The numerator in (6) represents the number of neutrons generated by neutron-induced fission and (n,2n) reactions, while the denominator denotes the number of neutrons lost by absorption reactions and leakage. The neutron leakage factor, ξ, is the fraction of neutrons that leak out from the core. It is estimated from the MCNP calculated neutron balance and assumed to be constant within a cycle.

2.2. FUEL CYCLE MODEL

After irradiation, the fraction *f* of the irradiated fuel is discharged. To describe the mass flow outside the reactor core, several vectors with different notations are introduced. The number of atoms of a nuclide discharged from the reactor core is expressed by the vector, $\vec{N}_{D,n}$, the number of atoms of a nuclide recovered from the discharged fuel by the vector, $\vec{N}_{R,n}$, the number of atoms of a nuclide in HLW by the vector, $\vec{N}_{W,n}$, the number of atoms of a nuclide in makeup material by the vector, $\vec{N}_{M,n}$, and the number of atoms of a nuclide in re-charged fuel by the vector, $\vec{N}_{C,n}$. $\vec{N}_{D,n}$ can be related to the vector, $\vec{N}_n(T_n^o + T_n)$ whose elements are the number of atoms of each nuclide in the reactor core at the end of *n*-th cycle as

$$\vec{N}_{D,n} = f\vec{N}_n(T_n^o + T_n). \tag{8}$$

The volume of the discharged fuel, V_D, is expressed as

$$V_D = fV, \tag{9}$$

where V is the volume of the fuel in the reactor before the discharge occurs and is assumed to be constant with time. In the partitioning stage, actinide atoms in the discharged fuel are recovered for the next cycle. Actinides that are not recovered, together with zirconium and all fission products in the discharged fuel are solidified and sent to the repository as HLW. Recovery fraction of element *e*, R_e, in the partitioning is defined as the ratio of the number of atoms of element *e* recovered from the discharged fuel to that in the discharged fuel before the partitioning occurs. Index *e* is used for numbering column in Figure 2. For example, all U isotopes are in column 1, all Np isotopes are in column 2, and so on. By mass balance,

$$\vec{N}_{D,n} = \vec{N}_{R,n} + \vec{N}_{W,n}. \tag{10}$$

We can write $\vec{N}_{R,n}$ and $\vec{N}_{W,n}$ as

$$\vec{N}_{R,n} = \mathbf{R}\vec{N}_{D,n}, \tag{11}$$

$$\vec{N}_{W,n} = (\mathbf{I} - \mathbf{R})\vec{N}_{D,n}, \tag{12}$$

where **I** is the unit matrix and **R** is the recovery fraction matrix. Elements of matrix **R** are all zero except for the diagonal elements. The diagonal elements are equal to the recovery fractions of corresponding elements. For example, the fifth diagonal element is equal to R_{Np}, which is the recovery fraction of ^{237}Np at the partitioning. By the assumption made at the beginning of this section, the isotopes of the same element have the same recovery fraction. For example, the first to the fourth diagonal elements correspond to the U isotopes in Figure 2. Therefore, these diagonal elements have the same value, R_U. The recovery fraction for element *e* satisfies $0 \le R_e < 1$.

In the fuel-fabrication facility, the recovered material inventory represented by the vector $\vec{N}_{R,n}$ is mixed with the makeup material inventory which is described by the vector $\vec{N}_{M,n}$. A fuel with $\vec{N}_{C,n}$ is fabricated, and loaded into the reactor core. By mass balance,

$$\vec{N}_{C,n} = \vec{N}_{R,n} + \vec{N}_{M,n}. \tag{13}$$

The volume, V_C, of the recharged fuel is assumed to be the same as that of the discharged fuel, V_D. By volume conservation,

$$V_C = V_{R,n} + V_{M,n}, \tag{14}$$

where $V_{R,n}$ is the volume of the recovered material, and $V_{M,n}$ is that of the makeup material. V_R is expressed as

$$V_{R,n} = \vec{\mu}^T \cdot \vec{N}_{R,n} , \tag{15}$$

where the elements of the vector, $\vec{\mu}$, are the reciprocals of the atomic density of nuclide i, and $\vec{\mu}^T$ is expressed as $\vec{\mu}^T = \{\rho_1^{-1}, \rho_2^{-1}, \rho_3^{-1}, ..., \rho_{18}^{-1}\}$.

The volume of makeup material, $V_{M,n}$, is the sum of the volume of actinides and that of zirconium. We set the volume fraction of actinides in the makeup material as ω. Then, the volume of actinides in the makeup material is $\omega V_{M,n}$. We determine ω in such a way that the recharged fuel has sufficiently high actinide content so that the whole core at the beginning of the next irradiation period has a k_{eff} value of 0.98. The makeup material consists of actinides and zirconium taken from LWR-spent fuel. The atom fraction, x_i, of actinide nuclide i in the makeup material is assumed to be constant. Then,

$$\omega V_{M,n} = N_{tot,M,n} \sum_i \frac{x_i}{\rho_i}, \qquad 0 \le \omega \le 1 . \tag{16}$$

The total number of atoms, $N_{tot,M,n}$, of actinides in the makeup material at the n-th cycle and the number, $N_{i,M,n}$, of atoms of an actinide nuclide i in the makeup material are related by

$$N_{tot,M,n} \equiv \sum_i N_{i,M,n} \quad \text{and} \quad N_{i,M,n} = x_i \sum_i N_{i,M,n} . \tag{17}$$

The volume of zirconium in the makeup material, $(1-\omega)V_{M,n}$, can be written as

$$(1-\omega)V_{M,n} = \frac{N_{Zr,M,n}}{\rho_{Zr}} , \tag{18}$$

where ρ_{Zr} is the atomic density of zirconium.

The number of fuel atoms at the beginning of the (n+1)-st cycle is determined by summing the fuel remaining in the reactor core and the recharged fuel and

$$\vec{N}^o_{n+1} = (1-f)\vec{N}_n(T_n^o + T_n) + f\mathbf{R}\vec{N}_n(T_n^o + T_n) + \vec{N}_{M,n} \tag{19}$$

obtained by substituting (8), (11) into (13). The vector $\vec{N}_{M,n}$ is yet to be determined. For this, the aforementioned k_{eff} constraints and the characteristics of actinide taken from the LWR-spent fuel are used. The value of k_{eff} of the reactor at the beginning of each irradiation period is set to be 0.98. Then, k_{eff} at the beginning of the (n+1)-st cycle must satisfy (6),

$$\frac{\sum_i \eta_i N^o_{i,n+1} \overline{\sigma}_{i,a}}{\xi\left(\sum_i N^o_{i,n+1}\overline{\sigma}_{i,a} + N^o_{F,n+1}\overline{\sigma}_{F,a} + N^o_{Zr,n+1}\overline{\sigma}_{Zr,a} + \sum_P N_P \overline{\sigma}_{P,a}\right)} = 0.98 . \tag{20}$$

The left side is the k_{eff} value at the beginning of the (n+1)-st cycle. By (19) and (17), the number of atoms of an actinide i in the reactor at the (n+1)-st cycle is written as

$$N^o_{i,n+1} = (1-f)N_{i,n}(T_n^o + T_n) + fR_e N_{i,n}(T_n^o + T_n) + x_i N_{tot,M,n} . \tag{21}$$

The number of fission-product pairs in the reactor at the (n+1)-st cycle is written as

$$N^o_{F,n+1} = (1-f)N_{F,n}(T^o_n + T_n)\,. \tag{22}$$

Using (18) and (16), the number, $\tilde{N}^o_{Zr,n+1}$, of atoms of zirconium in the reactor at the beginning of the (n+1)-st cycle is given by

$$\begin{aligned} N^o_{Zr,n+1} &= (1-f)N_{Zr,n}(T^o_n + T_n) + N_{Zr,M,n} \\ &= (1-f)N_{Zr,n}(T^o_n + T_n) + \rho_{Zr}V_{M,n} - \rho_{Zr}N_{tot,M,n}\sum_i \frac{x_i}{\rho_i}\,. \end{aligned} \tag{23}$$

Substituting (21), (22), and (23) into (20) yields an equation for $N_{tot,M,n}$. The value of $N_{tot,M,n}$ is obtained by solving that equation. By (16), the volume fraction, ω, of actinides in the makeup material at the n-th cycle and the number, $N_{i,M,n}$, of atoms of an actinide nuclide i can be determined. Once $N_{i,M,n}$ is known, $\tilde{N}_{M,n}$ is determined also. The number, $N_{Zr,M,n}$, of atoms of zirconium in the makeup material at the n-th cycle is obtained by (18).

3. BENCHMARKING AGAINST MOCUP

A computer code, WACOM, has been developed to implement the model described in section 2. To check WACOM, it has been benchmarked against MOCUP [4], a code package that couples MCNP [7] for particle transport calculations and ORIGEN 2 [6] for isotope depletion calculations. A proposed LBE-cooled blanket point design [1] has been used for benchmarking. Design parameters used are summarized in Table II.

Table II. Design Parameters for the Proposed LBE-Cooled Blanket Point Design [1]

Proton Energy (GeV)		1
Target Material		LBE
Fuel Material		(TRU-10Zr)-Zr
Pin Diameter (cm)		0.635
Cladding Thickness (cm)		0.056
Pitch-to-Diameter Ratio		1.727
Number of Pins per Assembly		217
Fuel Smear Density (%)		75
Volume Fraction (at operating temperature)	Fuel	0.140
	Structure	0.103
	Coolant	0.695
Hexagonal Assembly Pitch (cm)		16.142
Number of Assemblies	LBE target/buffer	19
	Fuel	192
	LBE Reflector	114
	Shield	66
TRU Fraction Split Factor (outer/middle/inner zone)		1.45/1.28/1.00
Active Fuel Height (cm)		106.68
Equivalent Fuel Region Diameter (cm)		246.21
Maximum Blanket Diameter (cm)		357.07
Number of Fuel Batches	Inner zone	5
	Middle and Outer Zones	6

Table III. Fuel Isotope Properties and PWR-TRU Composition [1][8][12]

i	Isotope	Atomic mass [amu]	Nominal density [g/cm^3]	Isotopic density [g/cm^3]	Weight fraction in TRU[a]	MPC for Ingestion [Ci/*l*]
1	U234	234.041	18.95	18.631	0.0000	3E-10
2	U235	235.044		18.811	4.0000E-05	3E-10
3	U236	236.046		18.891	2.0000E-05	3E-10
4	U238	238.051		19.052	4.7800E-03	3E-10
5	Np237	237.048	20.25	20.450	5.0230E-02	2E-11
6	Pu238	238.050	19.84	19.332	1.2720E-02	2E-11
7	Pu239	239.052		19.413	5.3196E-01	2E-11
8	Pu240	240.054		19.494	2.1534E-01	2E-11
9	Pu241	241.057		19.576	3.7820E-02	1E-09
10	Pu242	242.059		19.657	4.6850E-02	2E-11
11	Am241	241.057	13.67	13.557	8.9670E-02	2E-11
12	Am242m	242.060		13.614	1.4000E-04	2E-11
13	Am243	243.061		13.670	9.2600E-03	2E-11
14	Cm242	242.059	13.67	13.236	0.0000	7E-10
15	Cm243	243.061		13.291	2.0000E-05	3E-11
16	Cm244	244.063		13.346	1.0400E-03	3E-11
17	Cm245	245.066		13.400	9.0000E-05	2E-11
18	Cm246	246.067		13.455	1.0000E-05	2E-11
	Zr	91.22	6.49	6.49		

[a] Corresponding to a 25 year cooled PWR-TRU assuming that 99.995% of the uranium is removed in the UREX process

Table IV. Neutronic Characteristics and Half-Lives of Fuel Isotopes

Isotope	$\sigma_{n,\gamma}$ [b]	$\sigma_{n,2n}$ [b]	$\sigma_{n,f}$ [b]	ν [#/fission]	$t_{1/2}$ [s] [8]
U234	5.7880E-01	1.7950E-04	3.7800E-01	2.405	7.7160E+12
U235	4.4400E-01	5.2420E-04	1.7190E+00	2.471	2.2201E+16
U236	3.7650E-01	3.7210E-04	9.4920E-02	2.370	7.3794E+14
U238	2.8810E-01	6.5290E-04	3.2440E-02	2.523	1.4097E+17
Np237	1.2880E+00	1.4700E-04	3.6120E-01	2.697	6.7487E+13
Pu238	6.2110E-01	2.0990E-04	1.1530E+00	2.955	2.7121E+09
Pu239	3.8720E-01	2.7820E-04	1.7230E+00	2.944	7.6948E+11
Pu240	4.1930E-01	1.1210E-04	4.1060E-01	2.865	2.0751E+11
Pu241	3.6950E-01	9.4600E-04	2.2920E+00	2.973	4.1628E+08
Pu242	3.8000E-01	2.9200E-04	2.9120E-01	2.874	1.1952E+13
Am241	1.7279E+00[a]	3.2160E-05	2.7870E-01	3.294	1.3630E+10
Am242m	3.0920E-01	5.3090E-04	3.5790E+00	3.334	4.4466E+09
Am243	2.1780E+00[a]	3.6090E-05	2.1760E-01	3.346	2.3242E+11
Cm242	2.5300E-01	8.4110E-06	1.4830E-01	3.510	1.4083E+07
Cm243	2.0380E-01	5.0510E-04	2.4780E+00	3.503	9.4608E+08
Cm244	7.1560E-01	1.7500E-04	4.6950E-01	3.535	5.7080E+08
Cm245	2.6560E-01	9.1730E-04	2.1630E+00	3.684	2.6806E+11
Cm246	1.9550E-01	2.3340E-04	2.8140E-01	3.560	1.5011E+11
Zr	1.9187E-02	6.1139E-05	—	—	—
Pseudo FP	2.0742E-01	—	—	—	—

[a] Excitation cross section included. — not applicable.

To obtain basic neutronic data of the proposed LBE-ATW system using MCNP [7], it is assumed that the reactor has a cylindrical geometry with three regions: the target region, the fuel region, and the reflector region. The inner region is a spallation target with a radius of 36.9 cm, the middle section is the homogenized fuel region with a radius of 123.1 cm, and the outer section is the reflector region with a radius of 152.8 cm. The homogenized fuel region of the LBE-ATW reactor is composed of three constituents: fuel, coolant, and structural material. The properties and composition of the fuel in the homogenized region are given in Table III.

The effective one group cross-sections of the ATW fuel have been calculated with MCNP for a fuel that has a 45 weight percent of HM and a 55 weight percent of Zr. Table IV shows the obtained effective one-group cross sections, average numbers of neutrons produced per neutron-induced fission, and half-lives of the fuel isotopes. For the fission product (FP), a pseudo cross section has been estimated under the assumption that the estimated neutron absorption rate by fission products in MOCUP is equal to the neutron absorption rate by fission products calculated from this model.

Table V. Composition and Properties of LBE-Coolant [13][14]

Isotope	Nominal density [g/cm^3]	Weight fraction in coolant	Atom fraction in coolant	σ_a [b]
Pb	11.34	4.45E-01	4.4711E-01	3.7649E-03
Bi-209	9.80	5.55E-01	5.5289E-01	3.3624E-03

Table VI. Composition and Properties of Structural Material HT-9 [15]

Element	Nominal density [g/cm^3]	Weight fraction in structure	Atom fraction in structure	σ_a [b]
Fe	7.87	8.55E-01	8.5310E-01	9.0054E-03
Cr	7.19	1.16E-01	1.2431E-01	1.5005E-02
Ni	8.90	5.0E-03	4.7464E-03	1.7739E-02
Mo	10.20	1.5E-02	8.7121E-03	1.0761E-01
Mn	7.43	9.0E-03	9.1286E-03	2.6807E-02

Table VII. Fractional Changes of Fuel Isotopes for Irradiation time of 1 year

Isotopes	MOCUP	WACOM	Relative difference
U234[a]	2.4779E+23	2.4782E+23	0.01%
U235	1.1303E+00	1.1304E+00	0.01%
U236	2.1522E+00	2.1447E+00	0.35%
U238	9.5655E-01	9.5647E-01	0.01%
Np237	7.9779E-01	7.9777E-01	0.00%
Pu238	1.7643E+00	1.7699E+00	0.32%
Pu239	7.4899E-01	7.4900E-01	0.00%
Pu240	1.0006E+00	1.0005E+00	0.01%
Pu241	9.3182E-01	9.2832E-01	0.38%
Pu242	1.0033E+00	1.0033E+00	0.00%
Am241	7.7279E-01	7.7430E-01	0.20%
Am242m	2.0488E+01	2.0501E+01	0.06%
Am243	9.5276E-01	9.5288E-01	0.01%
Cm242[a]	3.3372E+25	3.3481E+25	0.33%
Cm243	6.9254E+00	6.9373E+00	0.17%
Cm244	3.1975E+00	3.1994E+00	0.06%
Cm245	2.8720E+00	2.8717E+00	0.01%
Cm246	1.5125E+00	1.5120E+00	0.03%

[a] The number of atoms at the beginning of irradiation was assumed as 1E+00

The proposed ATW reactor has a lead-bismuth eutectic (LBE) as its coolant. The composition and properties of

LBE-coolant are shown in Table V. Cross section data have been obtained by MCNP calculations. The density of the LBE-coolant is assumed as 10.151 g/cc at the temperature of 475 ^{o}C.

Table VI shows the properties of HT-9, the structural material assumed for the reactor. The density of HT-9 is assumed to be 7.66 g/cm^3 at 475 ^{o}C.

Table VII compares the fractional changes of the fuel isotopes in the reactor after an irradiation time of 1year for a single cycle. The fractional change is obtained by dividing the number of atoms of each isotope at the end of irradiation by its number of atoms at the beginning of irradiation. A very good agreement is found between WACOM and MOCUP.

4. LBE POINT DESIGN ANALYSIS

To illustrate the capabilities of WACOM, this code has been applied to the analysis of the LBE-cooled point design. We assume that the reactor is operated at a constant power of 840 MWt and the neutronic data obtained from the fuel composition with a 45 weight % HM is used through all irradiation periods. The fuel composition at the beginning of each cycle (BOC) is determined so that k_{eff}=0.98 (see (20)). Fuel irradiation stops when the value of k_{eff} drops to 0.92. Actinides contained in the discharged fuel are recycled, whereas zirconium and fission products are not recycled. The fraction f is assumed to be 1/6. R_e=0.999 is assumed for actinides in the discharged fuel.

Figure 3 shows the change of HM fraction of the fuel in the reactor core with the cycle number while Figure 4 shows the corresponding change of cycle duration. The inventory keeps increasing in order to maintain k_{eff}=0.98 at BOC. The addition of actinides is needed to compensate for the reactivity loss due to the variation in the actinide isotopic composition as well as for the buildup of fission products, shown in Figure 5. The HM loading in the fuel rods increases from 18.5 weight % at BOC to 36.5 weight % for the 200th cycle. The cycle duration correspondingly increases from ~81 days to ~220 days.

Figure 5 shows the evolution of the fuel isotopes inventory. Most nuclides inventory has a zigzag pattern within a cycle. The difference between the top and the bottom points represents the amount of the nuclide transmuted in the given cycle. ^{237}Np, ^{239}Pu and ^{241}Am have relatively high fractional transmutation per cycle.

Figure 6 shows the change of fractional transmutation in the reactor with cycle number. *Fractional transmutation is defined as the ratio of the difference between the amount of an isotope in the fuel at BOC and that at EOC to that at BOC within a cycle*. Positive values mean that the amount of an isotope increases during the cycle and negative values imply that the amount of an isotope decreases during the cycle. As observed in Figure 6, we can see that ^{237}Np, ^{239}Pu, and ^{241}Am have relatively large negative fractional transmutations, whereas other isotopes show buildup in the reactor at early cycles even though they eventually approach to zero, which means no depletion or accumulation of that nuclide in the fuel by recycling.

Figure 7 shows the cumulative waste reduction ratio of the ATW system. *The cumulative waste reduction ratio is defined as the cumulative amount of an isotope up to the n-th cycle in the waste stream divided by the cumulative amount of the same isotope up to the n-th cycle fed to the ATW system in the makeup stream*. The ratio means to what extent an isotope inventory can be reduced by the ATW system after a certain number of cycles. A small reduction ratio is desirable. The inventory of ^{239}Pu, ^{237}Np, and ^{241}Am is reduced by a factor of 1000 whereas the inventory of other Pu isotopes, ^{238}U, and ^{243}Am is reduced by a factor of 100 to 1000. The inventory of most of the Cm isotopes, ^{235}U, ^{236}U, and ^{242m}Am is reduced by a factor of 10. However, we can hardly expect the reduction of ^{246}Cm by the ATW system with the operating condition assumed here. In Figure 7, ^{234}U and ^{242}Cm are not shown because they are assumed not to exist in the makeup material.

Figure 8 shows the cumulative toxicity reduction ratio with the cycle number. *The cumulative toxicity reduction ratio is defined as the toxicity of all nuclides up to n-th cycle included in the waste stream divided by that of all nuclides included in the makeup material*. This is a key measure[*] for reactor performance in terms of reducing

[*] The toxicity still does not measure hazards and risk of geologic disposal because it does not take into account the mechanisms by which the radionuclides could be transported to, and taken in by humans. For a more comprehensive

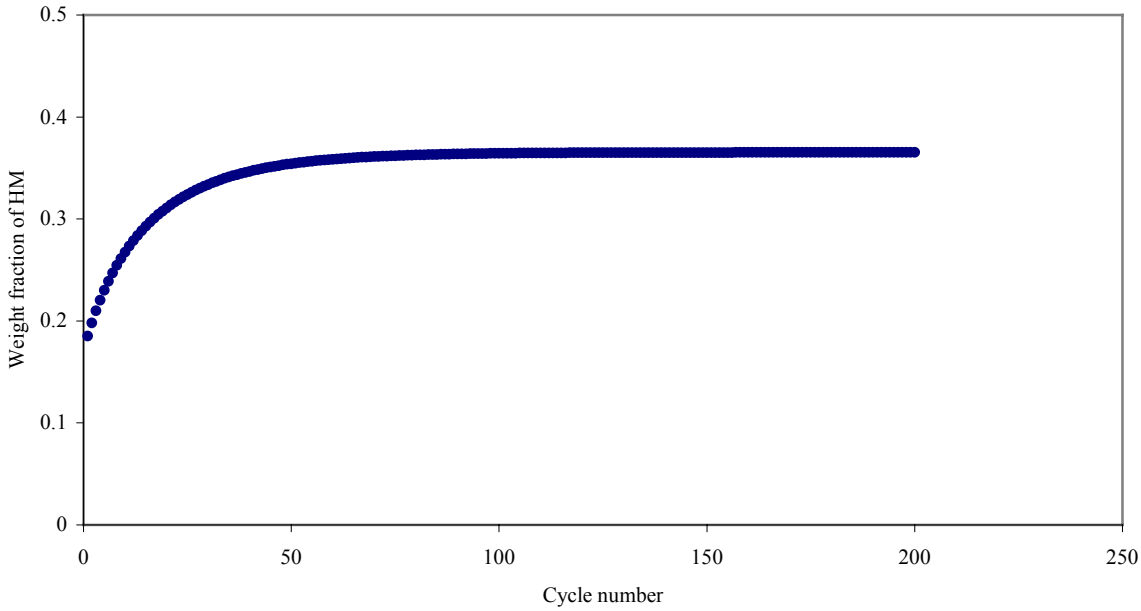

Figure 3. Cycle dependent HM fraction of fuel in the LBE reactor point design
(fuel discharge fraction = 1/6, actinide recovery fraction = 99.9 %)

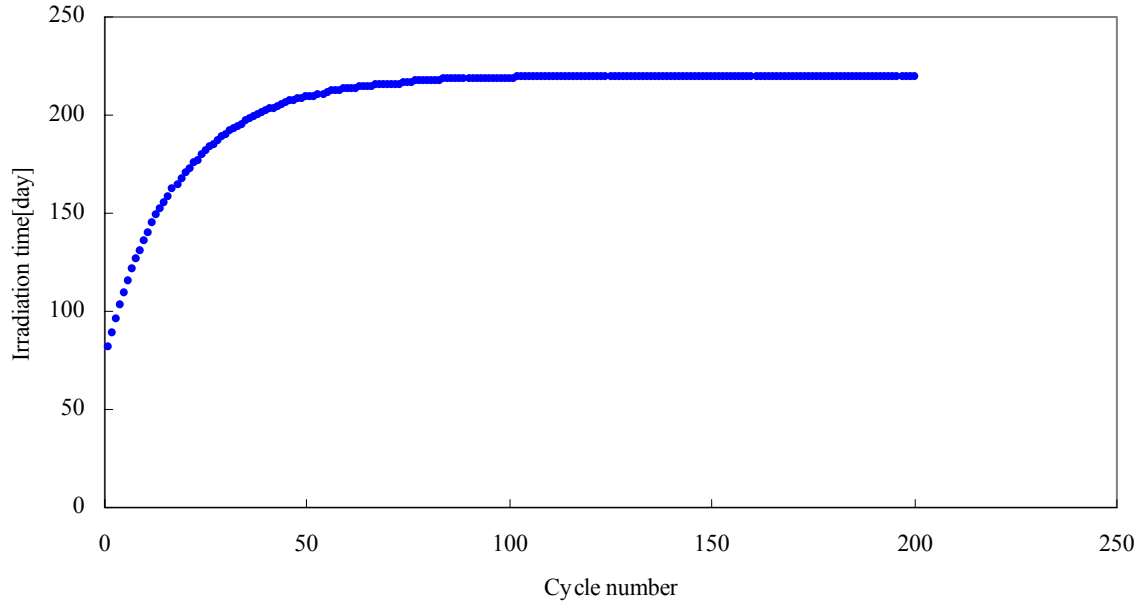

Figure 4. Evolution of irradiation time for the LBE reactor point design
(fuel discharge fraction = 1/6, actinide recovery fraction = 99.9 %)

comparison, the results of the present study should be used as input data for a repository performance assessment. Also, there would be other measures for repository impacts, such as the mass of weapons-usable material in a repository. Before comparing different designs and mode of operation of ATW systems, we need to express the results of the present analysis in terms of the repository impact measures.

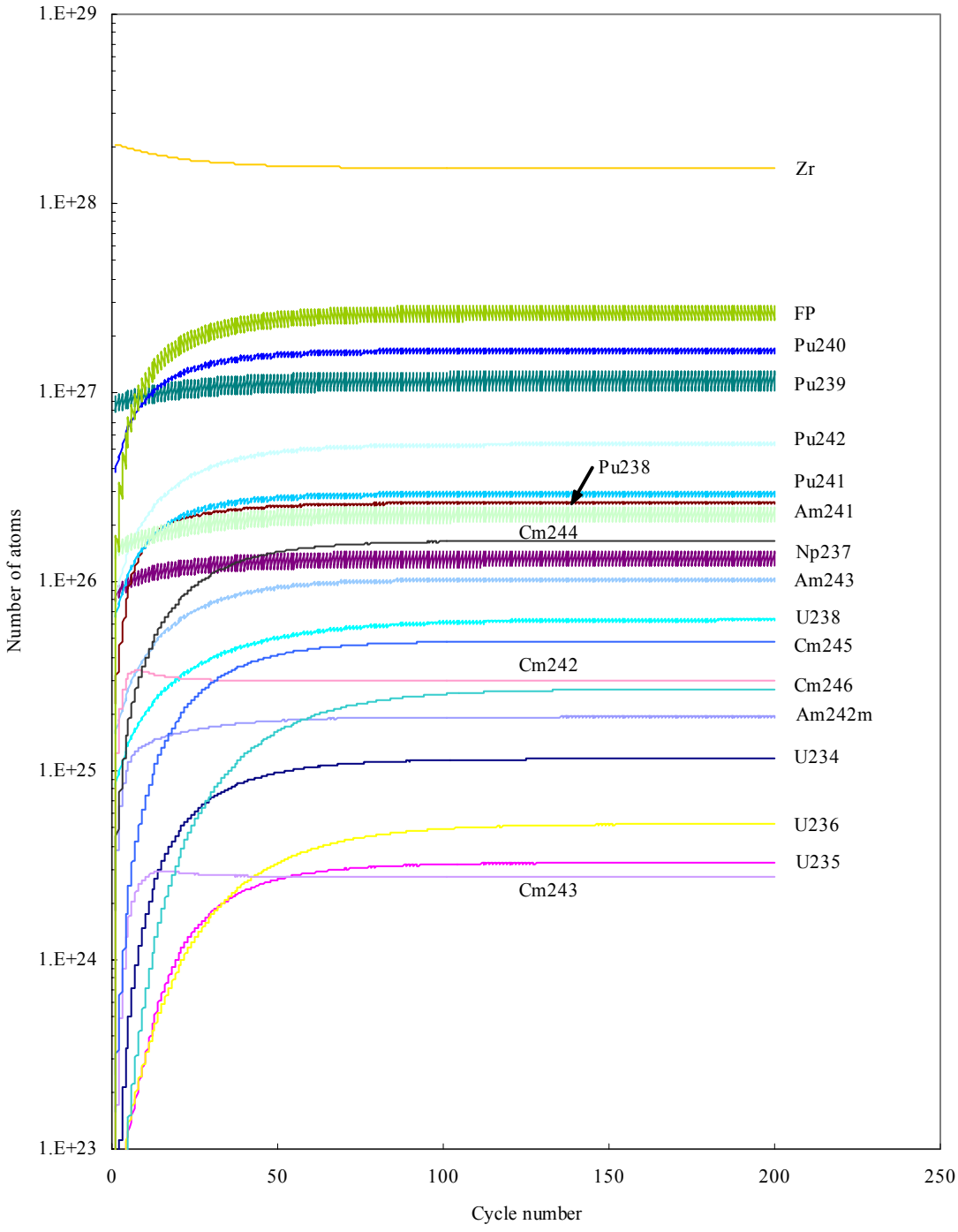

Figure 5. Cycle dependent in-core inventory of fuel isotopes in the LBE reactor point design (fuel discharge fraction = 1/6, actinide recovery fraction = 99.9 %)

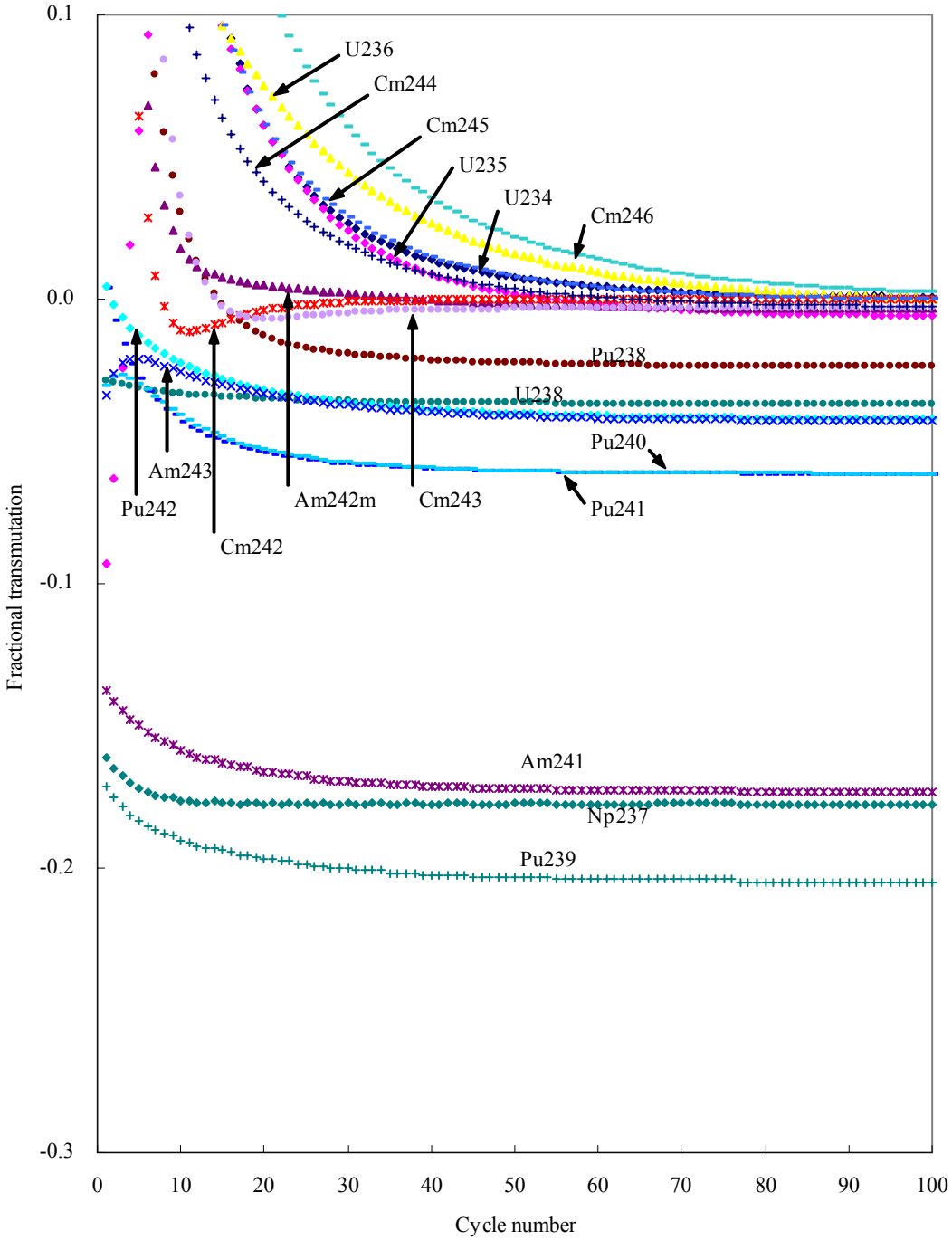

Figure 6. Fractional transmutation variation with cycle number
(fuel discharge fraction = 1/6, actinide recovery fraction = 99.9%)

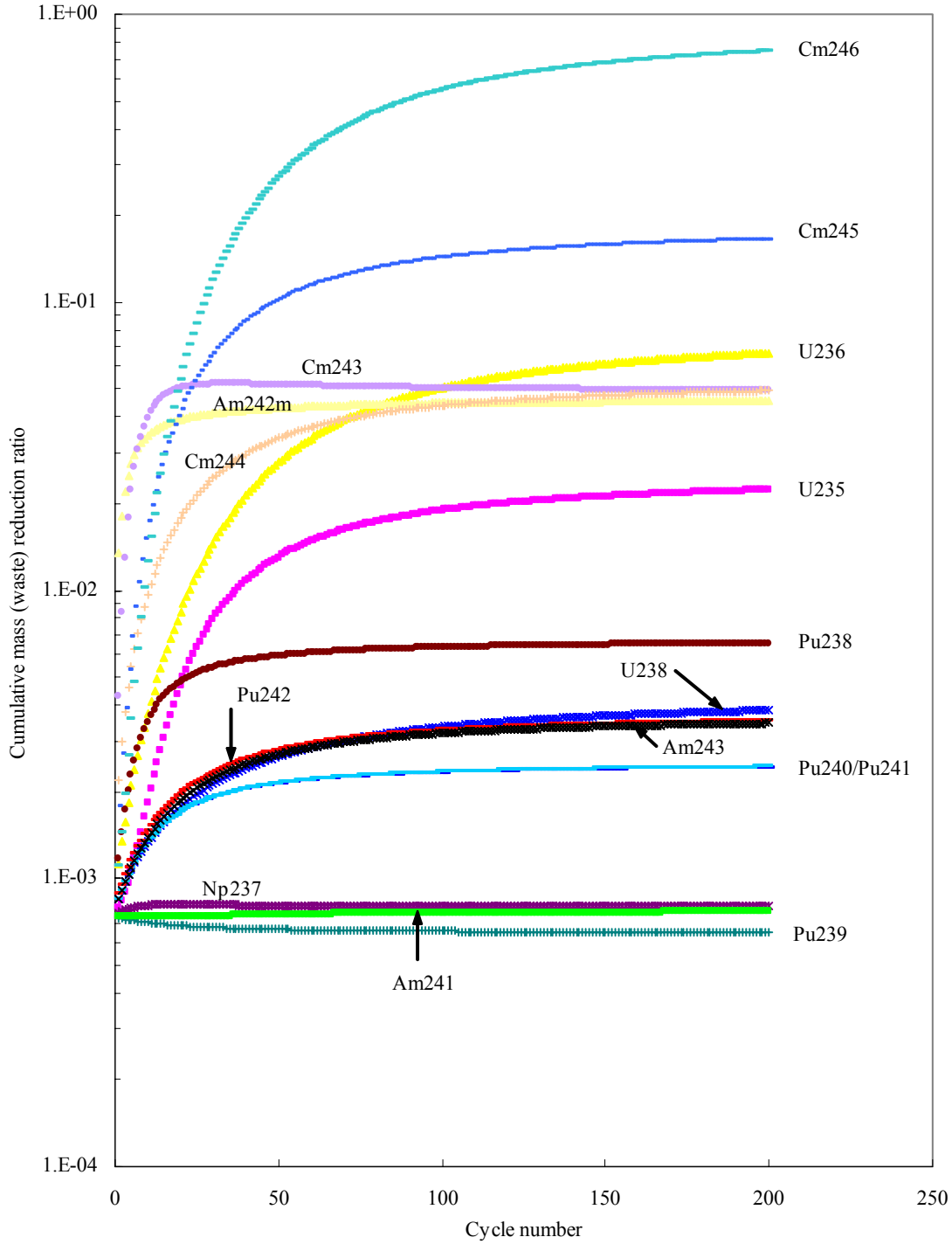

Figure 7. Cumulative waste reduction ratio with cycle number
(fuel discharge fraction=1/6, actinide recovery fraction=0.999)

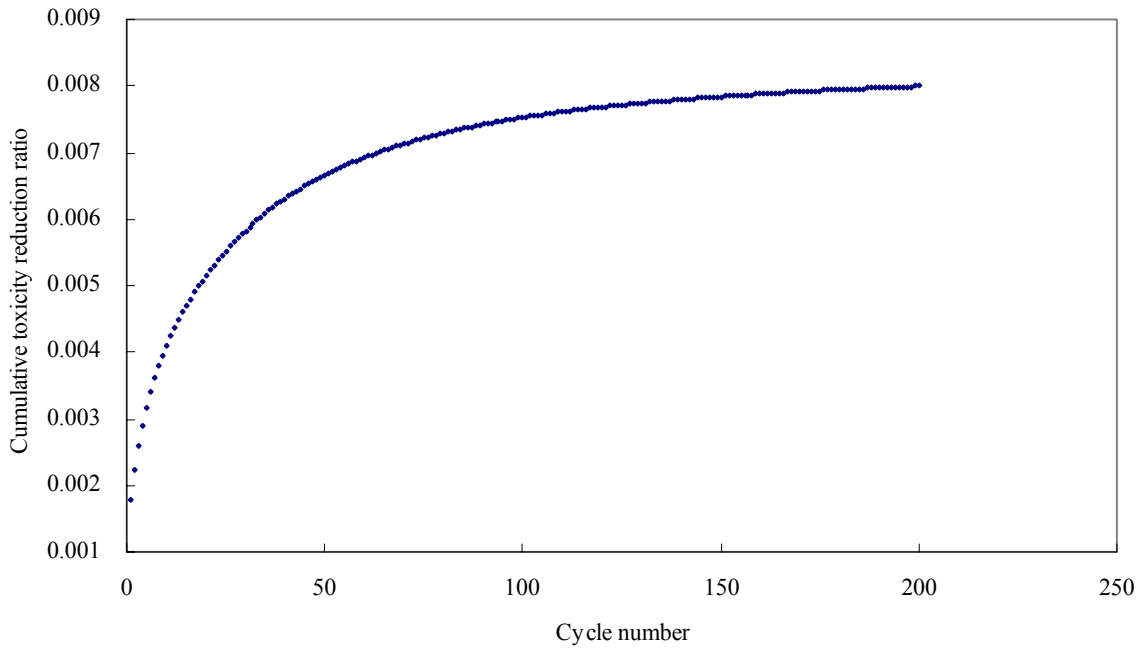

Figure 8. Cumulative toxicity reduction ratio with cycle number
(fuel discharge fraction=1/6, actinide recovery fraction=0.999)

hazard of radioactive materials. Figure 8 shows that the cumulative toxicity of actinides in the makeup stream can be reduced by a factor of 100 by the ATW system with the assumed operating conditions. The cumulative toxicity reduction ratio is dependent on various parameters of the ATW system.

Typical running time of WACOM for simulating the ATW system for 200 cycles is a few seconds on a Pentium III-500 PC.

CONCLUDING REMARKS

A simplified model and computer code has been developed for efficient simulation of the evolution of the fuel and waste composition and inventory in ATW systems, taking into account constraints on the reactor core design. The information that can be provided by the newly developed tool can be very useful for parametric studies of the impact of different transmutation systems design on the waste and repository assessment. Before applying the newly developed tool to actual analysis of transmutation systems it is necessary to work out an extension that will adjust the effective one group cross section and leakage factor to the variation in the HM loading and composition.

For the LBE-cooled transmuting reactor considered in this work the variation in the effective one group and leakage factor between the first cycle and "equilibrium" cycle is found to be within 20%. An algorithm will be developed for the WACOM code to linearly interpolate the cross sections and leakage factor between two data vectors to be generated with MCNP for the first cycle and nearly equilibrium cycle. Using this algorithm the number of cycles required for the HM inventory to reach equilibrium will be smaller than predicted in the illustration presented in Sec. 4. Thus, whereas Figures 3 and 4 predict that it will take ~50 cycles for the LBE ATW to reach a semi-equilibrium state, it is estimated that the number of cycles will be reduced to ~35 when using core composition dependent cross sections and leakage probability.

The toxicity reduction has been calculated as an example of a reactor performance measure for waste reduction. By the system considered, it has been shown that the toxicity of actinides included in LWR spent fuel would be reduced by a factor of hundred.

ACKNOWLEDGMENT

This work was supported by the U. S. Department of Energy Office of Nuclear Energy, Science, and Technology through the Los Alamos National Laboratory under contract number 14631-001-00 2K.

REFERENCES

[1] AAA-RPO-SYS-01-0008, LA-UR-01-1817, "Compendium of Initial System Point Designs for Accelerator Transmutation of Radioactive Waste", February 2001.
[2] D. Hill, *et al*., "A Roadmap for Developing ATW Technology: Systems Scenarios & Integration", ANL/RE-99/16, September 1999.
[3] B. J. Toppel, "A User's Guide for the REBUS-3 Fuel-Cycle-Analysis Capability", ANL-83-2, Argonne National Laboratory, (1983).
[4] R. L. Moore, B. G. Schnitzler, C. A. Wemple, R. S. Babcock, and D. E. Wessol, "MOCUP: MCNP-ORIGEN2 Coupled Utility Program", Idaho National Engineering Laboratory, (1995).
[5] D. L. Poston and H. R. Trellue, "User's Manual, Version 2.0 for MONTEBURNS Version1.0," "LA-UR-99-4999, September 1999.
[6] RSICC Code Package CCC-371, "ORIGEN 2.1-Isotope Generation and Depletion Code Matrix Exponential Method", (1999).
[7] RSICC Code Package CCC-700, "MCNP4C, Monte Carlo N-Particle Transport Code System", April 2000.
[8] Nuclear Data Evaluation Lab., Korea Atomic Energy Research Institute: "Table of the Nuclides", http://atom.kaeri.re.kr, (2000).
[9] A. G. Croff, "ORIGEN2: A Versatile Computer Code for Calculating the Nuclide Compositions and Characteristics of Nuclear Materials", *Nuclear Technology*, **Vol. 62**, September 1983.
[10] S. C. Chapra and R.P. Canale, "*Numerical Methods for Engineers*", McGraw-Hill, (1998).
[11] C. R. Wylie and L. C. Barrett, "*Advanced Engineering Mathematics*", 6th Edition, McGraw-Hill, (1995).
[12] U.S. Nuclear Regulatory Commission, NRC regulations(10CFR): "Appendix B", http://www.nrc.gov/reading-rm/doc-collections/cfr/part020, (2002).
[13] Bruce W. Spencer, "The Rush to Heavy Metal Reactor Coolants-Gimmick or Reasoned", *Proc. 8th Intl. Conf. on Nuclear Engineering*, ICONE8, Baltimore, MD, USA, April 2-6, 2000.
[14] "*Liquid Material Handbook*", 23rd ed., the Atomic Energy Commission, Department of Navy, Washington, D.C., (1952).
[15] IAEA-TECDOC-1039, "Influence of High Dose Irradiation on Core Structural and Fuel Materials in Advanced Reactors", June 1997.